УДК 551.515.6

doi: 10.31857/S2076673420030049

The relationship between methane transport to the atmosphere and the decay of the Kara Sea ice cover: satellite data for 2003–2019

L.N. Yurganov

University of Maryland Baltimore County, Baltimore, USA

Yurganov@umbc.edu

Связь между переносом метана в атмосферу и разрушением ледяного покрова Карского моря: спутниковые данные за 2003–2019 гг.

© 2020 г. Л.Н. Юрганов

Мэрилендский университет, Балтимор, США

Yurganov@umbc.edu

Received February 3, 2020 / Revised April 12, 2020 / Accepted June 7, 2020

Keywords: ***Arctic climate, greenhouse gases, methane, satellite data, sea ice.***

Summary

Satellite spectrometers operating on the outgoing long-wave IR (thermal) radiation of the Earth and placed in sun-synchronous polar orbits provide a wealth of information about Arctic methane (CH_4) year-round, day and night. Their data are unique for estimating methane emissions from the warming Arctic, both for land and sea. The article analyzes concentrations of methane obtained by the AIRS spectrometer in conjunction with microwave satellite measurements of sea ice concentration. The data were filtered for cases of sufficiently high temperature contrast in the lower atmosphere. The focus is on the Kara Sea during autumn-early winter season between 2003 and January 2019. This sea underwent dramatic decline in the ice cover. This shelf zone is characterized by huge reserves of oil and natural gas (~90% methane), as well as presence of sub-seabed permafrost and methane hydrates. Seasonal cycle of atmospheric methane has a minimum in early summer and a maximum in early winter. During last 16 years both summer and winter concentrations were increasing, but with different rates. Positive summer trends over the Kara Sea and over Atlantic control area were close one to another. In winter the Kara Sea methane was growing faster than over Atlantic. The methane seasonal cycle amplitude tripled from 2003 to 2019. This phenomenon was considered in terms of growing methane flux from the sea. This high trend was induced by a fast decay of the sea ice in this area with ice concentrations dropped from 95 to 20%. If the current Arctic sea cover would decline further and open water area would grow then further increase of methane concentration over the ocean may be foreseen.

Citation: Yurganov L.N. The relationship between methane transport to the atmosphere and the decay of the Kara Sea ice cover: satellite data for 2003–2019. *Led i Sneg*. Ice and Snow. 2020. 60 (3): 423–430. doi: 10.31857/S2076673420030049.

Поступила 3 февраля 2020 г. / После доработки 12 апреля 2020 г. / Принята к печати 7 июня 2020 г.

Ключевые слова: ***климат Арктики, метан, морской лед, парниковые газы, спутниковые данные.***

Проанализированы ИК спутниковые данные о концентрации метана в слое атмосферы 0–4 км над Карским и Баренцевым морями в сравнении с микроволновыми спутниковыми измерениями ледяного покрова Карского моря. За последние 16 лет амплитуда сезонных вариаций метана над северной частью Карского моря выросла в 3 раза, а площадь поверхности того же района, свободная от льда, увеличилась в 4 раза. Сделан вывод о значительной роли ледяного покрова в экранировании потока метана в атмосферу.

Introduction

The Arctic has experienced the fastest warming on the Earth over recent decades with the Arctic Ocean warming at nearly double the rate of the world's oceans [1]. The area of ice cover, its thickness and concentration have been significantly reduced [2]. There is concern about release of huge reserves of climate-active greenhouse gas methane (CH_4) in hydrates, permafrost and other reservoirs [3]. The radiation warming potential of methane is 28–34 times that of carbon dioxide (CO_2) over a 100-year time horizon [4]. The Barents and Kara seas (BKS) have extensive proven reserves of oil and natural gas [5]. Thermogenic methane seeps through sedimentary layers and forms hydrates at and below the seafloor. A review article [3] describes the principal processes that regulate methane distributions in the Arctic seafloor sediments, its fate in the water column, and subsequent release to the atmosphere. Enhanced dissolved methane concentrations in the seawater are likely. They are related, at least in part, to melting of gas hydrates and submerged permafrost. Methane is slowly oxidized by methanotrophic bacteria in deep layers with time-scales of weeks or years [6]. As it was concluded by [3], effects of reduced sea-ice cover on methane emissions to air are especially poorly constrained. Satellite data presented here allow to fill this gap.

Warm Atlantic currents make the BKS a climatically important region. A decline in BKS sea ice in early winter influences synoptic processes in the rest of the Northern hemisphere [7]. The Barents Sea is a shallow sea (average depth 230 m) with depressions up to 400 m. The Kara Sea is even shallower (average depth 100 m). One can expect release of methane from the seabed as a result of degradation of the submarine permafrost [8] in the Kara and southern Barents Seas. The Barents Sea is mostly free of ice year-round, while the Kara Sea winter ice cover underwent dramatic decline during early winters in 2000s [9].

Presence of sources is just one condition for methane to enter the atmosphere; a transport of the gas from the sea floor to the surface is equally important. The relatively warm and salty layer of Atlantic water (pycnocline) plays a role of a natural barrier for the penetration of methane into the surface layer of the sea in summer/early autumn between May and October [10]. Numerous direct studies have shown that during this season the flux in the Barents-Svalbard area is negligible [11–13]. These field investigations, however, discover strong sources at the seabed and huge concentrations of dissolved methane in deep waters. The flux of methane may be significant only after a breakdown of the pycnocline in November and deepening of the Mixed Layer. The Mixed Layer Depth (MLD) in the Arctic summer does not exceed 50 m. It increases sharply since November and, finally, the bulk of the Barents Sea water column is mixed down by December [14]. Increased turbulent diffusion induces methane emission to the atmosphere [15]. Methane over the Kara Sea was measured by IASI (Infrared Atmospheric Sounding Interferometer) [16]. A significant increase of methane from 2010 to 2016 was found for late autumn/winter season in BKS. A further AIRS-based (Atmospheric InfraRed Sounder) study [17] reported large positive methane anomalies around Franz Josef Land and offshore West Novaya Zemlya. Satisfactory explanations for significant positive trends in methane were not found.

Ice cover, like the pycnocline, plays the role of a natural barrier to methane. A degradation of sea ice [3] may increase methane flux and its atmospheric concentration. Satellite observations in the thermal IR range are extremely useful for characterizing methane over sea. They are especially helpful during the polar night, when space-borne Short-wave IR sensors (e.g., TROPOMI, that stands for TROPOspheric Monitoring Instrument) are useless and ship measurements are very difficult logistically. This paper analyzes methane concentrations in the lowest tropospheric layer over BKS delivered by AIRS between 2003 and 2019 with a focus on November-January period. These data were coupled with satellite microwave measurements of ice concentration. This area demonstrated the fastest decline in ice concentration for the entire Arctic Ocean in winter. The degradation of ice and increasing methane flux look like the most obvious explanation of the methane seasonal amplitude increase during last 16 years. Moreover, this allows one to expect further growth of methane emission from the Arctic Ocean, provided that the ice cover decay would proceed further.

Satellite data

The AIRS diffraction grating spectrometer was launched in a sun-synchronous polar orbit in May 2002 on board the Aqua satellite [18]. The instrument scans ±48.3° from the nadir, which provides full daily coverage in the Arctic. Spectral resolution is 1.5 cm^{-1} at the methane ν4 absorption band near 7.65 μm. Currently (April 2020), the AIRS is still operational. Starting in September 2002, methane data were processed using a single version 6 of the standard algorithm developed by NASA [19]. Monthly average Level 3 methane, surface and air temperatures between October 2002 and January 2020 are available on-line on a 1° × 1° latitude/longitude grid (AIRS3STM.006): https://disc.gsfc.nasa.gov/datasets/. Methane profiles were obtained for a 3 × 3 matrix of 9 pixels with a diameter of 13.5 km in nadir each. The profiles were averaged for the lower troposphere from the surface to the level of 600 hPa (~4 km). An empirical sensitivity to methane variations, 0.4–0.5, was based on comparison with simultaneous aircraft measurements at three stations in the United States [15]. A physical meaning of the sensitivity is a change in retrieved concentration that corresponds to the unit change of the «true» value. E.g., the sensitivity 0.5 means that real variations are underestimated by 100%. The Thermal IR reliable measurements require the surface to be warmer than air above it. The data were filtered for cases of Thermal Contrast ThC > 10 °C [20], where ThC = $T_{surf} - T_{600}$, T_{surf} is surface temperature, and T_{600} is air temperature at 600 hPa air pressure. Grey color in Fig. 3, *d* corresponds to areas with low ThC. So, vast areas of land and ice-covered ocean in winter can not be monitored using the current version of the processing technique.

Sea ice concentration data are archived by the NASA National Snow and Ice Data Center Distributed Active Archive Center (https://nsidc.org/data/NSIDC-0081/versions/1). The mean monthly data set [21] for 2003 – January 2019 is generated from the surface brightness temperature data and is designed to provide a consistent time series of sea ice concentrations C_{ice} (the fraction of ice for each 20 × 20 km^2 pixel) spanning the coverage of two passive microwave instruments developed as a part of the Defense Meteorological Satellite Program (DMSP), DMSP-F8 and Special Sensor Microwave Imager/Sounder (SSMIS) DMSP-F17. In our paper we use also the fraction of open water: $C_{wat} = 1 - C_{ice}$ for comparison with methane concentrations and their seasonal cycles.

Results

Methane in the mid-high Northern hemisphere has a maximum in winter and a minimum in summer. This cycle is driven mainly by seasonal changes in the tropospheric photochemical sink, a reaction of methane with hydroxil OH [22]. Hydroxil concentration has a winter minimum and a summer maximum; its source is also photochemical and requires ultraviolet solar radiation. Variations of hydroxil concentration with years are usually estimated as negligible or uncertain [23 and references therein]. Any changes of the methane seasonal cycle amplitude are supposed to be caused by changes in its sea-air flux after the November breakdown of the pycnocline [15]. Monthly mean low tropospheric methane concentrations for 2003–2019 in the Northern Kara Sea (Box 1, Svyataya Anna Trough) are plotted in Fig. 1, *a*. For comparison, a similar time series is presented for a control box between Iceland and Scandinavia (Box 2, see location of boxes on maps of Fig. 3), see Fig. 1, *b*. Least-squares linear regression lines were calculated separately for November–January (designated in what follows as «winter») and for April–July («summer»). The summer slopes are very close one to another, but the winter slope for the Kara Sea is significantly steeper. Amplitudes of the seasonal cycle (see Fig. 1, *c*) were calculated as a difference between winter and preceding summer averages. Parameters of regression for these and other cases are listed in Table.

The methane amplitudes in the Kara Sea grow with years, the amplitudes in a control Atlantic area also grow, but much slower (see Table). In fact, in 2003 the amplitudes of the methane cycle in these two places were the same, but in 2018 the amplitudes of methane in the Kara Sea were two to three times higher than in the Atlantic. A positive amplitude trend in the Kara Sea may be treated as a result of growing sea-air flux there due to a decline of the sea ice cover. To test this hypothesis, satellite data on ice concentration were used. Circles in Fig. 1, *c* are mean fractions of open water C_{wat} for the Box 1 (Kara Sea) for November–January in percent. Open water area in Northern Kara Sea almost quadrupled in 16 years. Corresponding methane seasonal cycle amplitude almost tripled. General trends are obvious, but inter-annual variations of both methane and open water in the Kara Sea are significant. It is natural to assume that many other atmospheric and oceanic processes are involved in these variability: the correlation coefficient R for methane and the open water area variations is not high (Fig. 2, see Table).

This part of the Arctic Ocean in winter time is unique in respect to the sea ice decline. This is illustrated by maps of mean open water fractions for periods: November 2003 – January 2004 (Fig. 3, *a*) and for November 2018 – January 2019 (see Fig. 3, *b*). Fig. 3, *c* is a simple difference between those two maps. Black continuous and dash lines correspond to ice edges, i.e., ice fraction (concentration) of 0.15. Fig. 3, *d* plots a distribution of late autumn/winter methane increase during last 16 years. A background methane concentration change (e.g., in Northern Atlantic) in 16 years may be estimated as 40–50 ppb. One should not forget, however, about a reduced sensitivity of satellite data to the lower troposphere, that tends to underestimate gas variation, see section «Satellite data» and [15]. Arctic methane increase in 16 years may be as high as 80 ppb, i.e., a contribution of the Arctic sources may be estimated as 30–40 ppb. Both long-term data (see Fig. 1) and comparison of maps for 2003 and 2018 (see Fig. 3) are consistent with an idea of ice cover decline as a reason for growing amplitude of the atmospheric methane concentration in northern parts of BKS.

Discussion

In our previous publication [15] IASI and AIRS methane data for the ice-free area to the South-West of Svalbard were analyzed. We found a good correla-

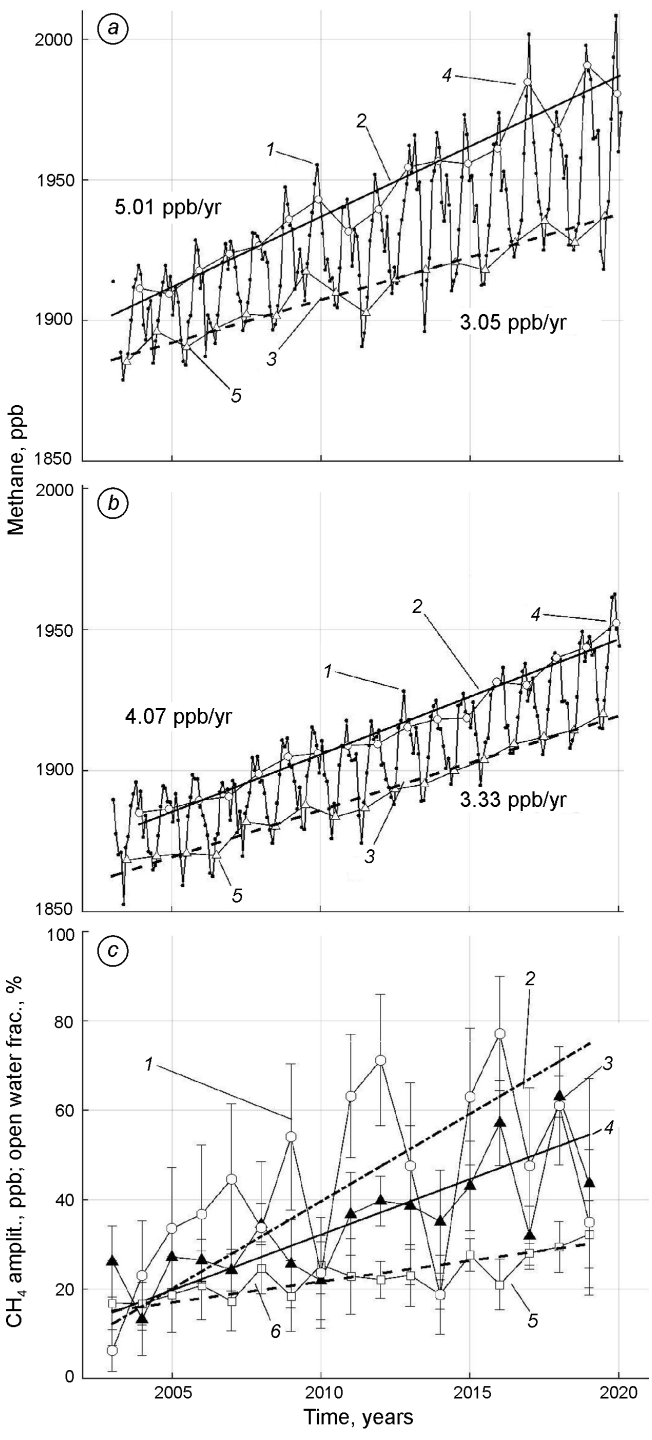

Fig. 1. Low troposphere (0–4 km of altitude) methane concentrations in N. Kara Sea and a control Atlantic domain. Ice-free fraction of the Kara Sea surface.

a – dots (*1*) are monthly mean methane for the Box 1 (Kara Sea). Solid line (*2*) is linear regression for periods November to January (winter). Dotted line (*3*) is linear regression for periods April to July (summer). Open circles (*4*) and open triangles (*5*) are for winter and summer seasonal averages, respectively. *b* – The same but for the control Box 2 (Northern Atlantic). *c* – Circles (*1*) are for open water fraction ($C_{wat} = 1 - C_{ice}$) for Box 1. Line *2* is linear regression. *3* and *5*- monthly mean amplitudes of seasonal cycles for Boxes 1 and 2, respectively. *4* and *6* – regression lines for methane amplitude, Boxes 1 and 2, respectively. Slopes are shown in Table

Рис. 1. Концентрации метана в нижней тропосфере (0–4 км по высоте) над севером Карского моря и над контрольным Атлантическим доменом. Относительная площадь поверхности, свободной ото льда, Карское море.

а – точки (*1*) – среднемесячные концентрации метана для домена 1; (*2*) – линейная регрессия для периода с ноября по январь (зима); (*3*) – линейная регрессия для периода с апреля по июль (лето); пустые кружки (*4*) и треугольники (*5*) для зимы и для лета соответственно. *b* – то же, но для контрольного домена 2 (Северная Атлантика). *с* – (*1*) – относительная площадь открытой воды ($C_{wat} = 1 - C_{ice}$) для домена 1 в процентах, Карское море; (*2*) – линейная регрессия; (*3*) и (*5*) – среднемесячные амплитуды сезонного цикла для доменов 1 и 2 соответственно; (*4*) и (*6*) – линии регрессии для доменов 1 и 2 соответственно. Наклоны линий регрессии приведены в таблице

tion between a seasonal course of methane monthly anomalies averaged over 2014–2016 and monthly MLD: after late October both methane and MLD increased. We connected this fact with the destruction of pycnocline in early November and increased turbulent diffusion. The water mixing is blocked by highly stratified seawater in summer. Changes in methane flux with years were not considered in that paper. Such analysis is conducted in the present study in regard to ice degradation in the Kara Sea. We found that during last 16 years a maximal trend of methane amplitude was observed over partially ice-covered Kara Sea (see Fig. 1–3 and see Table).

Mean autumn-winter ice concentration in the Northern Kara Sea (Box 1) diminished from ~95% in November 2003 – January 2004 to only ~20% in November 2016 – January 2017. This degradation of the ice cover significantly facilitated methane flux to air: the amplitude of the methane seasonal cycle for Box 1 increased from ~20 ppb to ~60 ppb. In fact, quadrupling open water area resulted in tripling methane cycle amplitude. During «normal» Kara Sea conditions, prevailed before early 2000s, most of methane emitted from the seafloor was oxidized by methanotrophic bacteria under the sea ice. Ice cover played the role of a lid that let bacteria to consume dissolved methane. Presently the situation is changing. The ice cover is declining, open water area is growing, the diffusion easily moves methane through the seawater column and numerous leads into the atmosphere. The diffusion seems to be faster than the bacterial oxidation that has timescales of weeks to months [6]. In a

Statistical parameters of linear regressions*
Статистические параметры линейной регрессии*

Line	Data and Box	Slope	Intercept	LCB	UCB	Corr. coeff.
1	Methane winter vs time, Box 1	5.01	−8129.61	4.3	5.72	0.93
2	Methane summer vs time, Box 1	3.05	−4220.35	2.53	3.57	0.90
3	Methane amplitude vs time, Box 1	2.49	−4967.72	1.63	3.34	0.60
4	Methane amplitude vs open water, Box 1	0.64	6.99	0.37	0.90	0.41
5	Methane winter, vs time Box 2	4.07	−6279.24	3.7	4.44	0.97
6	Methane summer vs time, Box 2	3.33	−4812.04	3.03	3.64	0.97
7	Open water vs time, Box 1	3.91	−7833.56	2.11	5.74	0.28

*LCB and UCB are lower and upper confidence bounds for slope at 95% confidence, calculated according to [29]. Units: lines 1–6, ppb/year or ppb. Line 7, percent/year or percent.
*LCB и UCB – нижняя и верхняя границы доверительного интервала для наклона [29]. Единицы измерения: строки 1– 6, ppb/год или ppb: строка 7 – процент/год или процент.

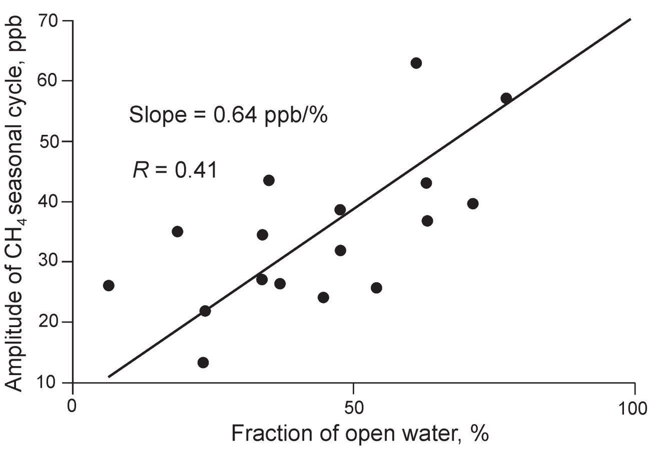

Fig. 2. Scattergram of methane cycle amplitude versus fraction of open water for Box 1 for 2003–2018
Рис. 2. Зависимость амплитуды сезонного цикла метана от относительной площади открытой воды для домена 1, 2003–2018 гг.

longer perspective, the sea ice may decline further and the winter ice degradation would expand to other Arctic seas. A further increase of methane flux from the Arctic Ocean surface may be expected. Satellite monitoring is important for elucidation of different factors influencing the methane cycle and trends.

A significant methane flux to atmosphere was reported for East Siberian Arctic Shelf seas [24], though later studies downplayed those high estimates, conclusions, and predictions [25, 26]. Unfortunately, reliable satellite data for this part of the Arctic in winter time are missing (grey areas on the map of Fig. 3, *d*). However, the influx of Pacific warm waters into the Chukchi Sea through the Bering Strait makes winter satellite measurements possible there too, but this area needs special consideration. Aircraft observations [27] in November, 2009, to the North of Bering Strait (2 circles in Fig. 3) showed a clear signature of methane flux from sea surface through leads. A discussion of the nature of methane sources is beyond the scope of this study; we discussed the role of modern changes in flooded permafrost and the seepage of thermogenic methane elsewhere [28].

Conclusions

1. We found that the amplitude of the methane seasonal cycle in the Northern Kara Sea tripled during the last 16-years period. The Kara Sea ice cover in the autumn-winter periods underwent crucial changes between 2003 and 2019: mean ice concentration diminished from 95% (2003/04 winter season) to 20% (2016/17 winter season) and open water area in November–January quadrupled. Ice cover plays a role of a barrier for methane. Its decline induces increase of the methane flux.

2. If the ice cover decay would proceed further, a growth of methane flux from the rest of the Arctic in late autumn/winter season is expected. In this regard our preliminary estimate of the Arctic Ocean methane contribution for 2010–2014 as ~2/3 of that from land [20] may be re-evaluated.

3. It's reasonable to assume that presently and in the near future ice cover decline would play a leading role for the methane trends in the Arctic, more important than deep seawater temperature changes. Growing methane in conjunction with warming seawater surface may induce positive feed-back link during winter with significant climatic consequences for populated mid-latitudes [7].

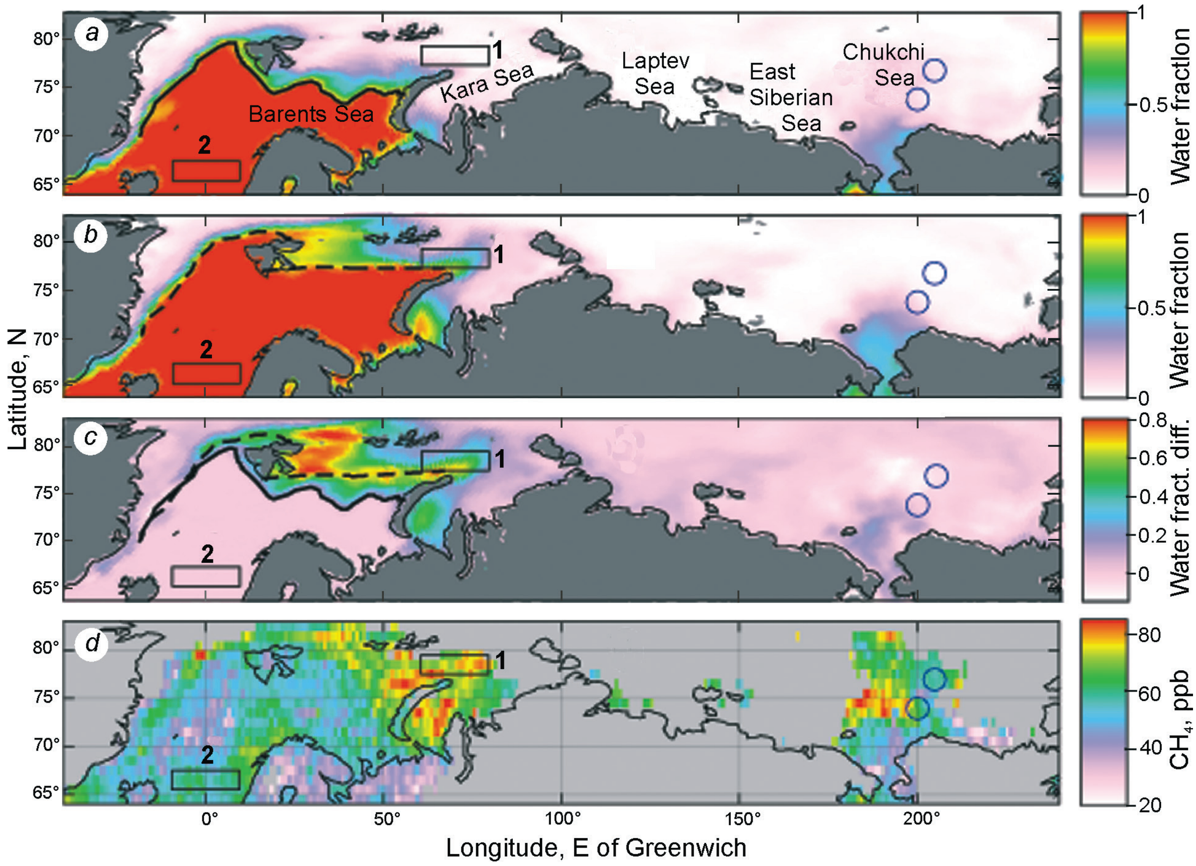

Fig. 3. Open water fraction C_{wat} and methane concentration change for the Russian Arctic shelf.

a – C_{wat} for November 2003 – January 2004; *b* – C_{wat} for November 2018 – January 2019; *c* – difference in water fraction between (*b*) and (*a*). The solid and dashed lines indicate the edge of the ice (ice concentration 15%). *d* – difference in low tropospheric methane concentration between winters of 2018/19 and 2003/04. Average depths for Boxes: 1 – 313 m; 2 – 2100 m

Рис. 3. Относительная площадь открытой воды C_{wat} и изменение концентрации метана для морей арктического шельфа России.

a – C_{wat} с ноября 2003 по январь 2004 г.; *b* – C_{wat} с ноября 2018 по январь 2019 г.; *c* – разница в относительной площади открытой воды между зимами 2003/04 г. и 2018/19 г., сплошная и штриховая линии обозначают кромку льда (концентрация льда 15%); *d* – разница концентраций метана в нижней тропосфере между зимами 2018/19 г. и 2003/04 г. Средние глубины для доменов: 1 – 313 м; 2 – 2100 м

Расширенный реферат

Метан (CH_4) – парниковый газ, второй по значению для глобального потепления после диоксида углерода (CO_2). Примерно половина источников метана в атмосфере имеет антропогенную природу и находится на континенте. Между тем, под шельфом Северного Ледовитого океана скрыты огромные запасы этого газа, который может выделяться в атмосферу по мере потепления Арктики. Метан просачивается из месторождений углеводородов, поступает из субаквальной мерзлоты и из метаногидратов. В результате парникового эффекта может возникнуть положительная обратная связь, которая приведёт к ускорению потепления. Измерения атмосферного метана над Северным Ледовитым океаном проводятся на судах и в процессе эпизодических самолётных экспериментов. Сложные климатические условия не позволяют вести такие работы в зимнее время. Спутники, запущенные на полярные солнечно-синхронные геоцентрические орбиты, дают возможность измерять газовый состав атмосферы, причём покрытие поверхности Арктики существенно лучше, чем в тропиках. Спектрометры, использующие солнечный свет (например, TROPOMI) по известным причинам в Арктике неэффективны, особенно во время полярной ночи. Для приборов, работающих на собственном ИК-излучении Земли и атмосферы, таких ограничений не существует.

В статье приведены данные об атмосферном метане над Северным Ледовитым океаном, полученные ИК-спектрометром AIRS в последние 16–17 лет. Исходные данные, обработанные НАСА, потребовали добавочной фильтрации для выделения случаев достаточно тёплой поверхности: разница между температурами поверхности и воздуха на высоте 4 км должна быть не менее 10 °C. Концентрации, усреднённые по слою 0–4 км высоты, были валидированы с помощью систематических самолётных измерений на трёх станциях НОАА в США. Чувствительность к изменениям концентрации метана в нижней тропосфере оценена в диапазоне 0,4–0,5 (отношение измеренной вариации метана к реальной). Кроме метана, использованы данные микроволновых спутниковых измерений концентрации льда (доли площади льда в пикселе 20 × 20 км^2). Доля чистой воды в домене сопоставлялась с вариациями концентрации метана. Потоки метана в атмосферу зависят от наличия источников метана на дне моря, в осадочных породах и/или в субаквальной мерзлоте. Второе условие для существования значительного потока газа в атмосферу – его перенос от глубоководных слоёв к поверхности. Летом существует естественный барьер для вертикального перемешивания водных масс – пикноклин, представляющий собой резкий скачок плотности воды на глубине ниже перемешенного слоя. Поток метана усиливается после разрушения пикноклина в ноябре. Но если поверхность воды в ноябре–декабре покрыта сплошным льдом, как это было до 2003 г. в Карском море, то его поток в атмосферу остаётся минимальным. Растворённый избыточный метан в течение зимы и лета окисляется бактериями.

Концентрации метана в период 2003–2019 гг. для севера Карского моря (жёлоб Святой Анны, домен 1 на рис. 3) и для контрольного района между Исландией и Скандинавией (домен 2) приведены на рис. 1, *a* и *b*. Сплошные линии показывают тренды изменения метана для сезонных максимумов и минимумов. Амплитуды сезонных вариаций для двух доменов нанесены в зависимости от времени на рис 1, *c*. Амплитуда сезонного хода метана над Карским морем существенно растёт с годами. Район Карского моря в начале зимы уникален для всего Северного Ледовитого океана с точки зрения тренда разрушения ледяного покрова: кружки на рис. 1, *c* соответствуют процентной доле площади открытой воды в домене 1. За 16 лет она возросла в 4 раза. Такой рост является рекордным для морей Северного Ледовитого океана (рис. 3, *a* – *c*). Рис. 3, *d* показывает пространственное распределение аномалий метана – разницу в концентрации между зимними сезонами 2003/04 и 2018/19 гг. Максимумы наблюдаются в Карском море, на северо-востоке Баренцева моря и на севере Чукотского моря. Серый цвет говорит об отсутствии надёжных данных. Результаты спутникового зондирования подтверждают предположение, что ледяной покров существенно блокировал поток метана от Карского моря в ноябре–январе в начале 2000-х годов, а его разрушение в последующие годы привело к росту амплитуды сезонного хода этого газа. Высказано мнение, что по крайней мере в ближайшем будущем рост потока метана от Северного Ледовитого океана будет в большей степени определяться процессом изменения ледяного покрова Арктики, чем изменениями температуры в глубине моря.

References

1. *Hoegh-Guldberg O., Bruno J.F.* The impact of climate change on the world's marine ecosystems. Science. 2010, 328: 1523–1528. doi: 10.1126/science.1189930
2. *Comiso J.C., Parkinson C. L., Gersten R., Stock L.* Accelerated decline in the Arctic sea ice cover. Geophys. Research Letters. 2008, 35: L01703. doi: 10.1029/2007GL031972.
3. *James R.H., Bousquet P., Bussmann I., Haeckel M., Kipfer R., Leifer I., Niemann H., Ostrovsky I., Piskozub J., Rehder G., Treude T., Vielstadte L., Greinert J.* Effects of Climate Change on Methane Emissions from Seafloor Sediments in the Arctic Ocean: A Review. Limnol. Oceanogr. 2016, 61: S283–S299. https://doi.org/10.1002/lno.10307.
4. *Myhre G., Shindell D., Bréon F.-M., Collins W., Fuglestvedt J., Huang J., Koch D. Lamarque J.-F., Lee D., Mendoza B., Nakajima T., Robock A., Stephens G., Takemura T., Zhang H.* Anthropogenic and natural radiative forcing. Climate Change 2013: The Physical Science Basis, Fifth Assessment Report of the Intergovernmental Panel on Climate Change. Eds.: Stocker T.F., Qin D., Plattner G.-K., Tignor M., Allen S.K., Boschung J., Nauels A., Xia Y., Bex V., Midgley P.M. Cambridge University Press, Cambridge, UK, New York, NY, USA, 2013: 659–740.
5. *Shipilov E.V., Murzin R.R.* Hydrocarbon deposits of western part of Russian shelf of Arctic—Geology and systematic variations. Petrol. Geol. 2002, 36 (4): 325–347. [Translated from Геология нефти и газа. 2001, 4: 6–19.]
6. *Reeburgh W.S.* Oceanic methane biogeochemistry. Chemical Reviews. 2007, 107: 486–513. doi: 10.1021/cr050362v.

7. *Petoukhov V., Semenov V.A.* A link between reduced Barents Kara sea ice and cold winter extremes over northern continents. Journ. of Geophys. Research. 2010, 115: D21111. doi: 10.1029/2009JD013568.
8. *Portnov A., Mienert J., Serov P.* Modeling the evolution of climate sensitive Arctic subsea permafrost in regions of extensive gas expulsion at the West Yamal shelf. Journ. of Geophys. Research. Biogeosciences. 2014, 119 (11): 2082–94. https://doi.org/10.1002/2014JG002685.
9. *Zhang Q., Xiao C., Ding M., Dou T.* Reconstruction of autumn sea ice extent changes since AD1289 in the Barents-Kara Sea, Arctic. China Earth Science. 2018, 61: 1279–1291. https://doi.org/10.1007/s11430-017-9196-4.
10. *Rudels B.* High latitude ocean convection. In: Flow and Creep in the Solar System: Observations, Modelling and Theory. Eds.: D.B. Stone and S.K. Runcorn. Academic Publishers, Dordrecht., 1993: 323–356.
11. *Gentz T., Damm E., von Deimling J.S., Mau S., McGinnis D.F., Schlüter M.* A water column study of methane around gas flares located at the West Spitsbergen continental margin. Continental Shelf Research. 2014, 72: 107–18 . doi: 10.1016/j.csr.2013.07.013.
12. *Myhre C.L., Ferré B., Platt S.M., Silyakova A., Hermansen O., Allen G., Pisso I., Schmidbauer N., Stohl A., Pitt J., Jansson P., Greinert J., Percival A.C., Fjaeraa M., O'Shea S.J., Gallagher M., Le Breton M., Bower K., N. Bauguitte S., J.B. Dalsøren S., Vadakkepuliyambatta S., Fisher R.E., Nisbet E.G., Lowry D., Myhre G., Pyle J.A., Cain M., Mienert J.* Extensive release of methane from Arctic seabed west of Svalbard during summer 2014 does not influence the atmosphere. Geophys. Research Letters. 2016, 43: 4624–4631. doi: 10.1002/2016GL068999.
13. *Mau S., Romer M., Torres M.E., Bussmann I., Pape T., Damm E., Geprags P., Wintersteller P., Hsu C.W., Loher M., Bohrman G.* Widespread Methane Seepage along the Continental Margin off Svalbard—From Bjornoya to Kongsfjorden. Sci. Rep. 2017, 7: 42997:1–42997:13. https://doi.org/10.1038/srep42997.
14. *Kara A.B, Rochford P.A, Hurlburt H.E.* Mixed layer depth variability over the global Ocean. Journ. of Geophys. Research. 2002, 108 (C3). doi: 10.1029/2000JC000736.
15. *Yurganov L., Muller-Karger F., Leifer I.* Methane increase over the Barents and Kara Seas after the autumn pycnocline breakdown: satellite observations. Adv. Polar Sci. 2019, 30 (4): 382–390. doi: 10.13679/j.advps.2019.0024.
16. *Yurganov L.N., Leifer I., Vadakkepuliyambatta S.* Evidences of accelerating the increase in the concentration of methane in the atmosphere after 2014: satellite data for the Arctic, Current problems in remote sensing of the Earth from space, 14 (5): 248–258. doi: 10.13140/RG.2.2.16613.29927.
17. *Leifer I., Chen F.R., McClimans T., Muller Karger F., Yurganov L.* Satellite ice extent, sea surface temperature, and atmospheric methane trends in the Barents and Kara Seas. The Cryosphere. Discussion. 2018. https://doi.org/10.5194/tc-2018-237.
18. *Xiong X., Barnet C., Maddy E., Sweeney C., Liu X., Zhou L., Goldberg M.* Characterization and validation of methane products from the Atmospheric Infrared Sounder (AIRS). Journ. of Geophys. Research. 2008, 113: G00A01. doi: 10.1029/2007JG000500.
19. *Susskind J., Blaisdell J.M., Iredell L.* Improved methodology for surface and atmospheric soundings, error estimates, and quality control procedures: the atmospheric infrared sounder science team version-6 retrieval algorithm. Journ. of Applied Remote Sensing. 2014, 8 (1): 084994. https://doi.org/10.1117/1.JRS.8.084994.
20. *Yurganov L., Leifer I., Lund-Myhre C.* Seasonal and interannual variability of atmospheric methane over Arctic Ocean from satellite data. Current Problems in Remote Sensing of Earth from Space. 2016, 13: 107–119. doi: 10.21046/2070-7401-2016-13-2-107-119.
21. *Cavalieri D.J., Parkinson C.L., Gloersen P., Zwally H.J.* Sea Ice Concentrations from Nimbus-7 SMMR and DMSP SSM/I-SSMIS Passive Microwave Data, Version 1. Boulder, Colorado USA. NASA National Snow and Ice Data Center Distributed Active Archive Center, 1996. doi: https://doi.org/10.5067/8GQ8LZQVL0VL.
22. *Holmes C.D., Prather M.J., Søvde O.A., Myhre G.* Future methane, hydroxil, and their uncertainties: key climate and emission parameters for future predictions. Atmospheric Chemistry and Physics. 2013, 13: 285–302. https://doi.org/10.5194/acp-13-285-2013.
23. *Stevenson D.S., Zhao A., Naik V., O'Connor F.M., Tilmes S., Zeng G., Murray L.T., Collins W.J., Griffiths P., Shim S., Horowitz L.W., Sentman L., Emmons L.* Trends in global tropospheric hydroxyl radical and methane lifetime since 1850 from AerChemMIP. Atmospheric Chemistry and Physics. Discussion. 2020. https://doi.org/10.5194/acp-2019-1219.
24. *Shakhova N., Semiletov I., Leifer I., Sergienko V., Salyuk A., Kosmach D., Chernikh D., Stubbs Ch., Nicolsky D., Tumskoy V., Gustafsson O.* Ebullition and storm-induced methane release from the East Siberian Arctic Shelf. National Geosciences. 2013, 7: 64–70. https://doi.org/10.1038/ngeo2007.
25. *Miller C.M., Dickens G.R., Jakobsson M., Johansson C., Koshurnikov A., O'Regan M., Muschitiello F., Stranne C., and Mörth C.-M.* Pore water geochemistry along continental slopes north of the East Siberian Sea: inference of low methane concentrations. Biogeosciences. 2017, 14 (12): 2929–2953. https://doi.org/10.5194/bg-14-2929-2017.
26. *Thornton B.F., Prytherch J., Andersson K., Brooks I.M., Salisbury D., Tjernström M., Crill P.M.* Shipborne eddy covariance observations of methane fluxes constrain Arctic sea emissions. Science Advances. 2020, 6 (5): eaay7934. doi: 10.1126/sciadv.aay7934.
27. *Kort E.A., Wofsy S.C., Daube B.C., Diao M., Elkins J.W., Gao R.S., Hintsa E.J., Hurst D.F., Jimenez R., Moore F.L., Spackman J.R., Zondlo M.A.* Atmospheric observations of Arctic Ocean methane emissions up to 82° north. National Geosciences. 2012, 5: 318–321. https://doi.org/10.1038/ngeo1452.
28. *Anisimov O.A., Zaboikina Y.G., Kokorev V.A., Yurganov L.N.* Possible causes of methane release from the East Arctic seas shelf. *Led i Sneg*. Ice and Snow. 2014, 54 (2): 69–81. https://doi.org/10.15356/2076-6734-2014-2-69-81. [In Russian].
29. *Chatterjee S., Hadi A.S.* Influential observations, high leverage points, and outliers in linear regression. Statistic Sciences. 1986, 1: 379–416.